Molecular Psychiatry
https://doi.org/10.1038/s41380-019-0492-3

ARTICLE

Dosage sensitivity intolerance of VIPR2 microduplication is disease causative to manifest schizophrenia-like phenotypes in a novel BAC transgenic mouse model

Xinli Tian[1] · Adam Richard[1] · Madison Wynne El-Saadi[1] · Aakriti Bhandari[1] · Brian Latimer[1] · Isabella Van Savage[1] · Kevlyn Holmes[2] · Ronald L. Klein[1] · Donard Dwyer[1] · Nicholas E. Goeders[1] · X. William Yang[3] · Xiao-Hong Lu[1]

Received: 29 July 2018 / Revised: 8 June 2019 / Accepted: 20 June 2019

Abstract

Recent genome-wide association studies (GWAS) have identified copy number variations (CNVs) at chromosomal locus 7q36.3 that significantly contribute to the risk of schizophrenia, with all of the microduplications occurring within a single gene: vasoactive intestinal peptide receptor 2 (VIPR2). To confirm disease causality and translate such a genetic vulnerability into mechanistic and pathophysiological insights, we have developed a series of conditional VIPR2 bacterial artificial chromosome (BAC) transgenic mouse models of VIPR2 CNV. VIPR2 CNV mouse model recapitulates gene expression and signaling deficits seen in human CNV carriers. VIPR2 microduplication in mice elicits prominent dorsal striatal dopamine dysfunction, cognitive, sensorimotor gating, and social behavioral deficits preceded by an increase of striatal cAMP/PKA signaling and the disrupted early postnatal striatal development. Genetic removal of VIPR2 transgene expression via crossing with Drd1a-Cre BAC transgenic mice rescued the dopamine D2 receptor abnormality and multiple behavioral deficits, implicating a pathogenic role of VIPR2 overexpression in dopaminoceptive neurons. Thus, our results provide further evidence to support the GWAS studies that the dosage sensitivity intolerance of VIPR2 is disease causative to manifest schizophrenia-like dopamine, cognitive, and social behavioral deficits in mice. The conditional BAC transgenesis offers a novel strategy to model CNVs with a gain-of -copies and facilitate the genetic dissection of when/where/how the genetic vulnerabilities affect development, structure, and function of neural circuits. Our findings have important implications for therapeutic development, and the etiology-relevant mouse model provides a useful preclinical platform for drug discovery.

Introduction

Copy number variations (CNVs) are a form of chromosomal structural variation that manifests as deletions or multiplications in the genome. As a source of genetic diversity, CNVs are abundant in the human genome [1]. Most CNVs are intergenic, small, or encompass genes that can tolerate a change in copy number, and are thus benign. However, several recent genome-wide association studies (GWAS) have identified multiple disease-associated, and likely causative CNVs, which have been convincingly shown to increase the risk of neurodevelopmental disorders, such as schizophrenia, autism spectrum disorder (ASD), intellectual disability, and attention-deficit-hyperactivity disorder [2]. The pathogenic consequences of CNVs have been proposed to include dosage sensitivity [3], or disruption of the genomic architecture, such as in repetitive elements, the creation of chimeric genes, or the disruption of functionally

Supplementary information The online version of this article (https://doi.org/10.1038/s41380-019-0492-3) contains supplementary material, which is available to authorized users.

✉ Xiao-Hong Lu
xlu1@lsuhsc.edu

[1] Department of Pharmacology, Toxicology and Neuroscience, Louisiana State University Health Sciences Center, Shreveport, LA 71130, USA

[2] California Lutheran University, Thousand Oaks, CA, USA

[3] Center for Neurobehavioral Genetics, Jane and Terry Semel Institute for Human Behaviors, Department of Psychiatry and Biobehavioral Sciences, David Geffen School of Medicine at University of California, Los Angeles, CA 90095, USA

Published online: 23 August 2019

clustered genes [4, 5]. Furthermore, most CNVs contain numerous genes and affect multiple organ systems and brain regions at different developmental stages. It is difficult to distinguish cell-type autonomy from systemic effects. There is currently a major gap in linking these candidate genetic vulnerabilities to dysfunctional neuronal subtypes and circuits. Etiology-relevant animal model and sophisticated genetic dissection are needed to confirm the disease causality of CNVs and to understand when/where/how CNVs affect the development, structure, and function of neural circuits. Such studies are necessary to gain insights into the mechanisms of disease pathogenesis and pathophysiology [6].

Recent large-scale GWAS studies pinpointed a CNV at the chromosomal locus 7q36.3 in schizophrenia patients at a rate 14 times higher than in healthy individuals in the European population, with all of the microduplications occurring within a single gene: VIPR2 [7, 8]. The association was later validated in a Han Chinese population [9]. In the latest and largest genome-wide searches of schizophrenia-linked CNVs performed by the Psychiatric Genomics Consortium, schizophrenia patients were reported to carry 11% more CNVs than controls. VIPR2 CNV was again identified as one of 17 significant CNV loci with a false discovery rate (BH-FDR) <0.05 [10]. Furthermore, in Vacic et al., VIPR2 CNV was also significantly overrepresented in ASD [7].

Indeed, genes and loci disrupted by pathogenic CNVs open a window to probe the key neurobiological mechanisms important to brain development and pathophysiology. The VIPR2 gene encodes the VPAC2 receptor, whose ligands are vasoactive intestinal peptide (VIP) and pituitary adenylate cyclase-activating peptide (PACAP). VIPR2 is a stimulatory canonical G-protein coupled receptor (GPCR) that activates adenylyl cyclase (AC)-cyclic adenosine 3′, 5′-mono-phosphate (cAMP)-protein kinase A (PKA) signal transduction. VIP and PACAP are neuropeptides that play an important role in neurodevelopment, cognition, circadian rhythm, emotion, and neuroinflammation [11]. Disruption of VIP signaling has been linked to autism, Down syndrome, and fetal alcohol syndrome [12]. Early postnatal activation of the VIPR2 receptor elicits profound neurodevelopmental deficits including synaptic changes and sensorimotor gating deficits [13]. VIPR2 is expressed in the cortex, striatum, hippocampus, olfactory bulb, thalamus, and suprachiasmatic nucleus (SCN), implying a pleiotropic role of VIP/VPAC2 signaling in brain function and development. It has been well established since 1980s, VIP robustly stimulates cAMP signaling in striatal neurons [14–18]. Based on the detailed characterization of VIP-induced neural signaling changes (e.g., cAMP-regulated phosphoproteins) in striatal neurons, Greengard proposed a neuromodulatory role of dopamine (DA) together with VIP acting at VIP receptors in striatal dopaminocetive neurons [16, 18] (Supplementary Fig. S1B). VPAC2 is the only VIP receptor in the striatum with high binding density, which is in contrast to the cortex where both VPAC1 and VPAC2 are expressed [19, 20]. Importantly, VIPR2 gene expression level in the striatum is moderate in comparison to other brain regions, suggesting striatal expression is critically regulated and vulnerable to an increase of gene dosage.

Originating from Eugen Bleuler's "splitting mind" and "4 A's", schizophrenia has been viewed as a collection of behavioral phenotypes resulting from "disconnectivity" of the brain's anatomic regions and functional pathways. Longstanding evidence implicates the role of brain regions such as the prefrontal cortex, hippocampus, and thalamus in the pathophysiology of schizophrenia. However, recent neuroimaging studies had unanticipated findings that DA abnormalities in schizophrenia are the greatest within dorsal, especially associative striatum [21]. Associative striatum receives convergent inputs from multiple cortical regions to integrate cognitive and affective processes and has been implicated in schizophrenia pathophysiology [21–23]. Mouse genetics has also shown that overexpressing dopamine D2 receptor only in the striatum could elicit cortical hypofunction and cognitive deficits [24], suggesting a primary striatal abnormality. The vast majority of neurons in the striatum are GABAergic spiny projection neurons (SPNs). As shown in Fig. S1, SPNs are divided into two subpopulations, the direct pathway SPN (dSPN) expressing Gs-coupled dopamine D1 receptors that send axons directly to the internal segment of the globus pallidus (GPi) and the substantia nigra pars reticulata (SNr), and the indirect pathway SPN (iSPN) expressing Gi-coupled D2 receptors, as well as Gs-coupled adenosine A2a receptor, that send axons indirectly to the SNr via the external segment of the globus pallidus (GPe) and subthalamic nucleus. Intracellular signaling cascades operating in these two types of SPNs, especially striatal PKA [25] is positively regulated by Gs-coupled D1 or A2a or VPAC2 and negatively regulated by Gi-coupled D2 receptors. PKA signaling is important for modification of neuronal excitability, synaptic neuroplasticity, and excitatory synaptogenesis in early postnatal striatal development [26]. Thus, it is conceivable that genetic or environmental factors, e.g., excessive VIP/VPAC2 signaling that disrupts striatal PKA signaling would contribute to a wide range of striatal dysfunction and derail the developmental trajectory of the early assembly of striatal circuits and its connectivity with other brain regions.

Therefore, the overall goal of this study is to develop an etiology-relevant animal model of one of the CNVs associated with schizophrenia to (1) provide further evidence to support the disease causality; and (2) translate the genetic vulnerability into mechanistic and pathophysiologic insights. We have developed a conditional human VIPR2

CNV bacterial artificial chromosome (BAC) transgenic mouse model that recapitulates the genetic architecture of the susceptibility allele, which, therefore, satisfies construct validity [6]. Furthermore, the conditional design of the BAC allows switching-off the transgene in desired spatiotemporal patterns, controlled by Cre recombinase, thus facilitating dissection of the inflicted neurocircuits. Human VIPR2 microduplication elicits persistent and prominent dorsal striatal DA dysfunction, consistent with recent human neuroimaging studies that DA abnormalities in schizophrenia are the greatest within dorsal striatum as opposed to the mesolimbic pathway. VIPR2 CNV mice also manifest cognitive, sensorimotor gating, and social behavioral deficits that are preceded by an increase of striatal cAMP/PKA signaling, striatal neuron dendritic deficits, and disrupted early postnatal development (Supplementary Table S1). Our compelling evidence further supports a causal pathogenic role of VIPR2 gene dosage sensitivity in the disruption of the developmental trajectory of striatal neurocircuits with the manifestation of behavioral deficits. The genetic dissection experiment starts to shed light on the pathogenic role of VIPR2 overexpression in dopaminoceptive neurons and the manifestation of DA and behavioral deficits of schizophrenia.

Materials/subjects and methods

Generation of BAC transgenic mice

A 210-kb mouse BAC (CTD-3011O24) containing the VIPR2 genomic sequence was identified through a database search and obtained from the BACPAC resource center (Oakland Children's Hospital, Oakland). LoxP sites were inserted into exon 1 of the human VIPR2 gene preceding the endogenous translation initiation codon according to an established BAC modification protocol. Maxiprep DNA was prepared from the modified VIPR2 BACs and purified using cesium prep. DNA was separated on a pulsed field gel to select the fractions with intact BAC DNA. The intact BAC DNA fraction was selected and microinjected into fertilized FvB mouse zygotes to generate BAC transgenic mice at Cyagen. Genotyping and copy number primers were listed in Supplementary Table S2.

Quantitative real-time PCR

For all quantitative real-time PCR (qPCR) experiments, VIPR2 CNV animals were euthanized by cervical dislocation. RNA was purified using Direct-zol RNA purification kits (Zymo research). qPCR analyses were performed on a Roche LightCycler 480 using the Roche LightCycler FastStart DNA MasterPLUS SYBR Green I mix (Roche Diagnostics, Mannheim, Germany). All samples were run in triplicate. GAPDH was used to normalize the overall cDNA content of all samples.

Behavioral analysis

T-maze spontaneous alternation, delayed non-matched-to-place (DNMTP) task, social interaction, and social recognition in three chamber test, and prepulse inhibition (PPI) test were described in the Supplementary Methods.

cAMP ELISA assay

cAMP levels were measured using a complete ELISA assay according to the manufacturer's directions (Enzo Life Sciences, Farmingdale, NY, USA). Supernatant fractions of the tissue were prepared by centrifugation at $14{,}000 \times g$ for 30 min at 4 °C.

Whole-animal bioimaging of the CRE-Luc mice

Mice were anesthetized with isoflurane and injected subcutaneously with 250 mg/kg D-luciferin (Xenogen, Alameda, CA) dissolved in Dulbecco's phosphate-buffered saline without Ca^{2+} or Mg^{2+}. Seven minutes after the luciferin injection, mice were placed in the IVIS Lumina (Xenogen) and imaged with 1-min exposures every 5 min for 120 min. The field of view was set at B, binning set to 2; f-stop set at 1.2. Pseudocolor bioluminescent images were superimposed onto photographic images of the mice and analyzed using the Living Image 3.0 software (Xenogen).

Western blot analysis, immunofluorescence, immunohistochemistry (IHC), and imaging

Western blot analysis, histology, immunofluorescence, IHC, and imaging were performed using the established protocol and were described in the Supplementary Methods. The antibodies, source, research resource identifiers, and dilutions can be found in the Supplementary Table S3.

High-performance liquid chromatography (HPLC) for determination of DA and other neurotransmitters in brain tissue

HPLC was performed using the established protocol and the detailed method was described in the Supplementary Methods.

Experimental design and statistical analysis were described in detail in the Supplementary Methods.

Results

Genomic copies and gene expression phenotypes of VIPR2 BAC transgenic mice

We have engineered a 231-kb BAC (CTD-3011O24) containing human VIPR2 locus (116 kb), with an 84 kb 5′ flanking and a 14 kb 3′ flanking genomic region, and with no other full-length gene on the BAC (Fig. 1a). Importantly, the first exon of VIPR2, which contains the endogenous translation initiation codon, was flanked by two LoxP sites. The LoxP sites are located in the 5′ untranslated region and intron one flanking VIPR2 exon 1. Thus, these LoxP sites do not interfere with the expression of VIPR2 but do allow for Cre-mediated excision of hVIPR2 exon 1. As a result, the VIPR2 CNV model is designed to be a conditional inactivation model in which Cre can switch off the transgene expression in desired temporal and spatial patterns controlled by crossing with mice expressing Cre recombinase (Fig. 1a). We confirmed that the VIPR2 BAC was correctly modified by using two sets of primers that flank the modification regions (Supplementary Fig. S2A). Maxiprep DNA was prepared from the modified VIPR2 BAC and purified through cesium prep. The purified DNA was

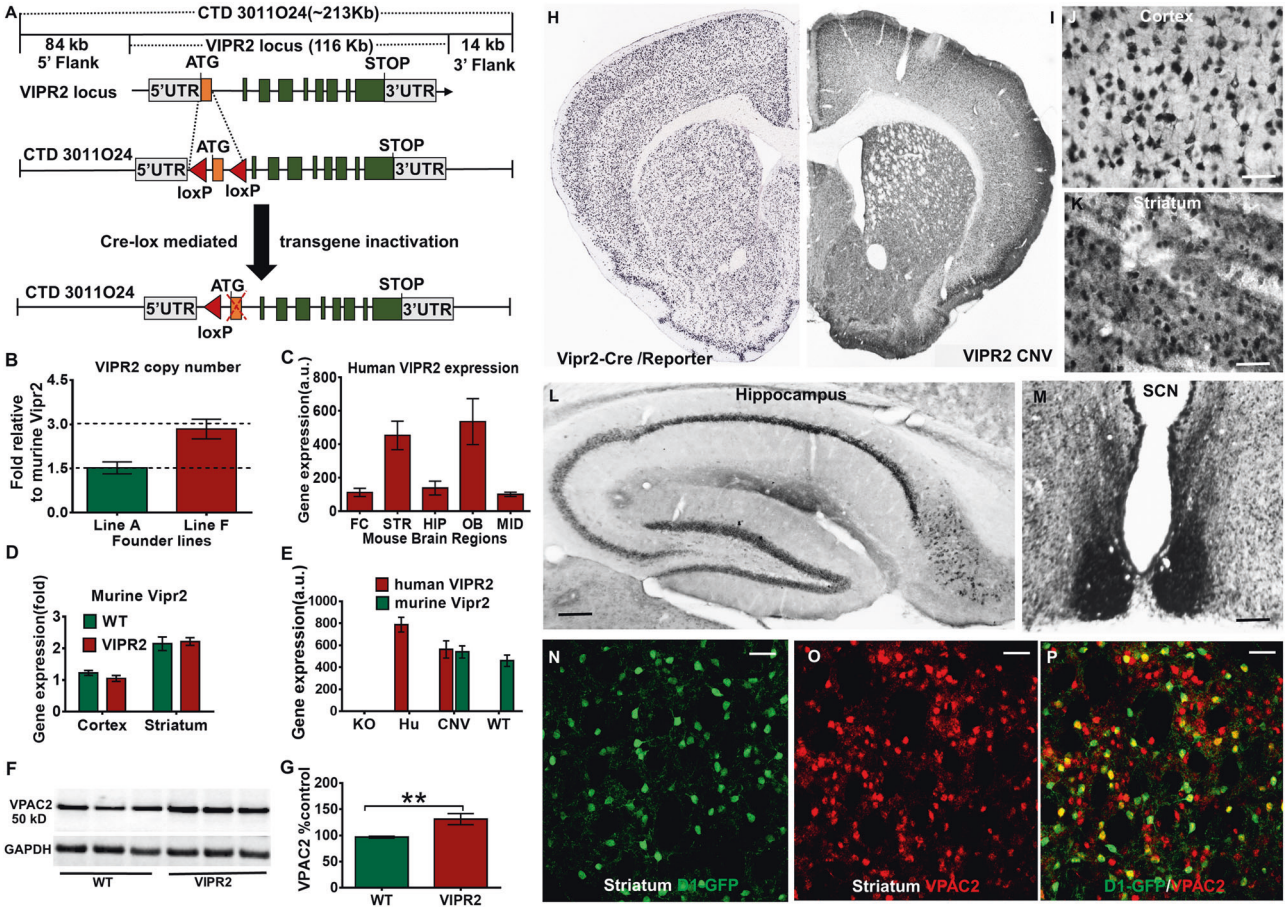

Fig. 1 Human VIPR2 copy number and gene expression in VIPR2 CNV BAC transgenic mice. **a** Design of conditional VIPR2 BAC transgenic mice. **b** Primers specific for both the human and mouse VIPR2 gene were used to quantify transgene copy numbers in VIPR2 CNV mice. Mouse wild-type genomic DNA was used as a two copy per diploid genome control. Line A contains one human copy of the VIPR2 genomic locus sequences (i.e., BAC transgene copies), and Line F contains four human transgene copies. **c** Relative expression of human VIPR2 mRNA in different brain regions of VIPR2 CNV mice (Line A) determined by qPCR analysis. FC frontal cortex, STR striatum, HIP hippocampus, OB olfactory bulb, MID midbrain. **d** Relative expression of human VIPR2 gene and endogenous mouse VIPR2 gene in cortex and striatum of VIPR2 CNV mice (Line A) determined by qPCR. **e** Endogenous murine VIPR2 and human VIPR2 transgene expression in mouse VIPR2 knockout (KO), fully humanized (Hu), VIPR2 CNV (Line A), and wild-type mice (WT) determined by qPCR. **f**, **g** Western blot of the VPAC2 protein in the striatum of VIPR2 CNV mice (Line A) and quantifications ($n = 4$–6, *t*-test, $^{**}p < 0.01$). Mouse VIPR2 expression as shown from the image of in situ hybridization (ISH) in the mouse VIPR2-BAC Cre mice crossing with reporter mice (Allen Brain Atlas) (**h**) and immunohistochemistry staining (**i**) to determine the human VIPR2 expression in the mouse VIPR2 null background. The expression of human VIPR2 was confirmed in the cortex (**j**), striatum (**k**), hippocampus (**l**), and the suprachiasmatic nucleus (SCN, **m**). **i**, **j** scale bar = 25 μm; **k** scale bar = 10 μm; **m** scale bar = 50 μm. **n**–**p** hVIPR2 is expressed in dSPNs in the striatum as demonstrated by the double fluorescence staining of GFP (green) and VPAC2 (red) in Drd1a-GFP/ VIPR2 CNV double transgenic mice (Line A). Scale bar = 25 μm

separated on a pulsed field gel to verify the integrity of the BAC (Supplementary Fig. S2B). The intact BAC DNA fraction was selected and microinjected into 200 fertilized FVB mouse zygotes to generate BAC transgenic mice.

Out of 54 pups born, we identified six positive transgenic founders using three different pairs of primers that are specific for the modification region (Supplementary Fig. S2C). The positive transgenic founders were bred with C57BL/6 J wild-type mice to maintain the lines. Further characterization using quantitative PCR identified multiple copies of human VIPR2 gene were integrated into the mouse genome (Fig. 1b). In transgenic founder Lines A and F, quantitative PCR analyses of the genomic DNA revealed that VIPR2 CNV mice have tandem integration of approximately one and four copies of the human VIPR2 transgene, respectively (Fig. 1b). Therefore, Line A is a model of hVIPR2 microduplication, and Line F, with four extra copies of the hVIPR2, can be used to study the gene dosage effects of hVIPR2 in mice. These two founder lines were characterized in detail.

To demonstrate that VIPR2 CNV mice express functional human VIPR2 transgene in an endogenous-like expression pattern in the mouse brain, we bred VIPR2 CNV mice (Line F, with four human copies) onto a mouse VIPR2 null background (B6.129P2 − VIPR2 < tm1Ajh > /J, JAX029215). Offspring from the breeding of fully humanized VIPR2 mice did not deviate from the expected Mendelian distribution. The humanized VIPR2 CNV mice were born with no observable gross anatomic or behavioral deficits up to 12 months of age. Furthermore, real-time quantitative reverse transcription PCR (qRT-PCR) analyses revealed that humanized VIPR2 mice expressed only human VIPR2 and not murine VIPR2 (Fig. 1e). We did not observe gross deficits due to a possible gain-of-toxic-function or haploinsufficiency. These results demonstrate that human VIPR2 transgene is properly expressed in mice and it retains the essential functions of mouse wild-type VIPR2. We are characterizing these mice as a fully humanized model to study human VIPR2 gene dosage and human VPAC2 receptor-specific antagonists.

Human VIPR2 transgene expression in mice

We have used qRT-PCR, western blot, immunostaining, and validated antibody in knockout and humanized mouse models to confirm that human VIPR2 is overexpressed in the VIPR2 CNV mouse models. First, the relative expression of human VIPR2 mRNA in different brain regions of VIPR2 CNV mice were determined by qRT-PCR analyses (Line A, Fig. 1c). Human VIPR2 mRNA is expressed in mouse frontal cortex, striatum, hippocampus, olfactory bulb, and hypothalamus. We found that human VIPR2 has a higher expression level in the striatum in comparison to the cortex (Line A, Fig. 1c). This is consistent with previous reports that in the rodent brain, the striatum contains many more VPAC2 receptors than other VIP/PACAP receptors as shown by in situ and qRT-PCR [20, 27–29]. The striatum also has the highest VPAC2 binding site density, as shown by autoradiography, but no VPAC1 [20]. In the founder Line A (microduplication model), the mRNA expression level of the human VIPR2 transgene and endogenous mouse gene are comparable in cortex and striatum (Fig. 1e), suggesting a twofold increase of total VIPR2 mRNA in the microduplication mice, which is consistent with the transcriptional changes seen in the lymphocytes from the VIPR2 duplication patients [7]. Furthermore, the human transgene does not affect the endogenous mouse gene expression in both cortex and striatum (Line A, Fig. 1d).

The antibodies to GPCRs are frequently nonspecific. It has been proposed that GPCR antibodies should be validated by the disappearance of staining in knockout animals of the target receptor [30]. We used the VPAC2 antibody (Abcam, ab28624) previously validated in knockout mice (the same knockout strain we used to generate the humanized mice) [31]. The antibody also has been widely used to study VIPR2 expression in mouse brain [32]. To further confirm that the human VIPR2 protein is overexpressed in the CNV mice and has the same expression pattern as the endogenous mouse VIPR2, we further performed antibody validation by IHC staining (1:30,000 dilution followed by Tyramide Signal Amplification) in the humanized VIPR2 mice (without endogenous mouse VIPR2 allele) and VIPR2 knockout mice. As shown in Supplementary Fig. S3A, we have confirmed that the antibody is specific, as the VIPR2 null mouse shows little or no VIPR2 immunoreactivity.

With IHC staining in the humanized mice, we found that human VIPR2 transgene had modest expression levels in the frontal cortex, striatum, and hippocampus, and a high expression level in the olfactory bulb and SCN (humanized line, Fig. 1h–m). The human transgene expression is almost identical to the expression of the endogenous mouse VIPR2 (Fig. 1h). The mouse endogenous VIPR2 gene expression has been characterized by Allen Brain Institute using VIPR2 BAC-Cre_KE2 Cre reporter mice generated using a mouse VIPR2 BAC from Gene Expression Nervous System Atlas (GENSAT) (Fig. 1h) [33]. Besides, Allen Brain Institute generated two additional VIPR2 Cre knockin reporter lines. All three reporter lines have been verified in detail at Allen Brain Institute using a tdTomato reporter mouse model, which provides a more sensitive readout [34]. Finally, GENSAT characterized the gene expression pattern of the BAC-VIPR2-Cre mice mouse and reported that the gene expression pattern of the BAC-VIPR2-Cre mice matches previously published in situ data. According to GENSAT, the Cre expression is in both direct and indirect pathway medium spiny neurons. We further confirmed that the

human VIPR2 transgene is expressed in both dSPNs and iSPNs using the double fluorescence staining in Drd1a-GFP/ VIPR2 transgenic mice (humanized line, Fig. 1n–p) and a D2 receptor antibody (Supplementary Fig. S3B). Furthermore, using IHC staining as shown in Fig. 1i, j, we found that both human and mouse VIPR2 have a membranous expression pattern in neuronal cell bodies and dendrites shown as neuropil staining. Finally, we validated the overexpression of VIPR2 protein by western blot using a human VIPR2 rabbit monoclonal antibody (Sigma MAB SP235, former Spring Bioscience). The specificity of the antibody also has been previously validated by preadsorption, transfected cells, and in knockout mouse brains [35, 36]. VIPR2 CNV mice (Line A) have an about 50% increase of protein level in the striatum (Fig. 1f, g). Thus, we demonstrated that human VIPR2 transgene is overexpressed in the VIPR2 CNV model.

Adult VIPR2 CNV BAC transgenic mice manifest cognitive, sensorimotor, and social deficits

Next, we assessed the behavior of adult VIPR2 CNV mice using tests designed to evaluate the locomotor activity, motor performance/skill learning, depression, cognition, sociability, and sensorimotor gating behavior. Two of the transgenic founder lines (A and F) were used for the behavioral analysis. All behavioral tests were carried out with age and gender-matched (both male and female) mice from 3–6 months of age. As shown in Supplementary Fig. S4A, B, both founder lines of the VIPR2 CNV mice displayed normal general locomotor activity in the open field assay compared with their wild-type littermate controls. VIPR2 CNV mice (both lines) did not display anxiety behavior as they spent comparable time in the marginal area as in center area (Supplementary Fig. S4C, D).

DNMTP task in T-maze for spatial working memory

We measured spatial working memory using a DNMTP task in T-maze (Fig. 2a) in both founder lines of the mice as described by Tamura et al. and others [37] and detailed in the "Materials/subjects and Methods" section. Mice were food deprived to 80–85% of their body weight followed by a maintenance diet throughout testing (Fig. 2a). Performance over training, as measured by an increase in the number of correct choices made, were analyzed by two-way repeated measure ANOVA. With repeated trials (ten trials per day), the wild-type mice showed less of a tendency to enter a previously visited arm. However, both founder lines of the VIPR2 CNV mice took significant longer time to reach criterion (70% of correct choice for 3 consecutive days) than the wild-type mice (Fig. 2b, c, repeated measure linear model ANOVA, Line A: $F(9, 126) = 3.184$, $p = 0.0017$ for interaction effect, $F(1, 18) = 4.390$, $p = 0.0548$ for genotype difference. Line F: $F(9, 162) = 2.353$, $p = 0.0160$ for interaction effect; $F(1, 18) = 6.036$, $p = 0.0244$ for genotype difference, wildtype: $n = 10$ mice; male: $n = 5$; female: $n = 5$; Line A: $n = 9$ mice; male: $n = 4$; female: $n = 5$; Line F: $n = 10$ mice; male: $n = 6$; female: $n = 4$), indicating a spatial working memory deficit.

In order to control for the potential confounding factor of food preference in the DNMTP task, we also measured the spatial working memory using spontaneous alteration task in T-maze (Fig. 2d). Two independent founder line cohorts (Lines A and F) of VIPR2 mice showed significantly less spontaneous alterations than control mice (one-way ANOVA, $F(2, 28) = 9.554$, $p = 0.0007$) with Turkey's post hoc test, Line A: $^{**}p < 0.001$; Line F: $^{\#\#}p < 0.001$. Wildtype: $n = 15$ mice; male: $n = 9$; female: $n = 6$; Line A: $n = 8$ mice; male: $n = 4$; female: $n = 4$; Line F: $n = 8$ mice; male: $n = 3$; female: $n = 5$), indicating the working memory deficits seen in DNMTP was not due to differences in food preference between genotypes.

Novel object recognition test

Recognition memory was also examined in the VIPR2 CNV mice using a novel object recognition test. Mice were presented with two identical objects during the first session, and then one of the two objects was replaced by a novel object during a second session. The amount of time taken to explore the new object provides an index of recognition memory. While the control mice showed a trend to interact more with the novel object, VIPR2 CNV mice founder Line A (but not founder Line F) showed a statistical significance to interact less with the novel object, suggesting recognition memory deficits (Supplementary Fig. S5, one-way ANOVA, with Turkey's post hoc test. Line A: $^{*}p < 0.05$. Wildtype: $n = 14$ mice; male: $n = 9$; female: $n = 5$; Line A: $n = 10$ mice; male: $n = 4$; female: $n = 6$; Line F: $n = 8$ mice; male: $n = 4$; female: $n = 4$).

Impaired sensorimotor gating in PPI test

PPI is a "cross-species" neurological phenomenon of sensorimotor gating. The reduced PPI has been proposed as a biomarker of schizophrenia [38]. An acoustic startle reflex measurement system was used (Med Associates, USA) [39] to measure PPI in the VIPR2 CNV mice and wild-type littermates at 3–5 months of age. Each test session consisted of four types of prepulse-pulse trials that included two different prepulse intensities (75 and 85 dB) and two different interstimulus intervals (30 ms and 100 ms), plus the startle pulse-alone trials that were pseudorandomized, with the background noise level in each chamber at 65 dB. For wild-type littermates, a weaker acoustic prestimulus

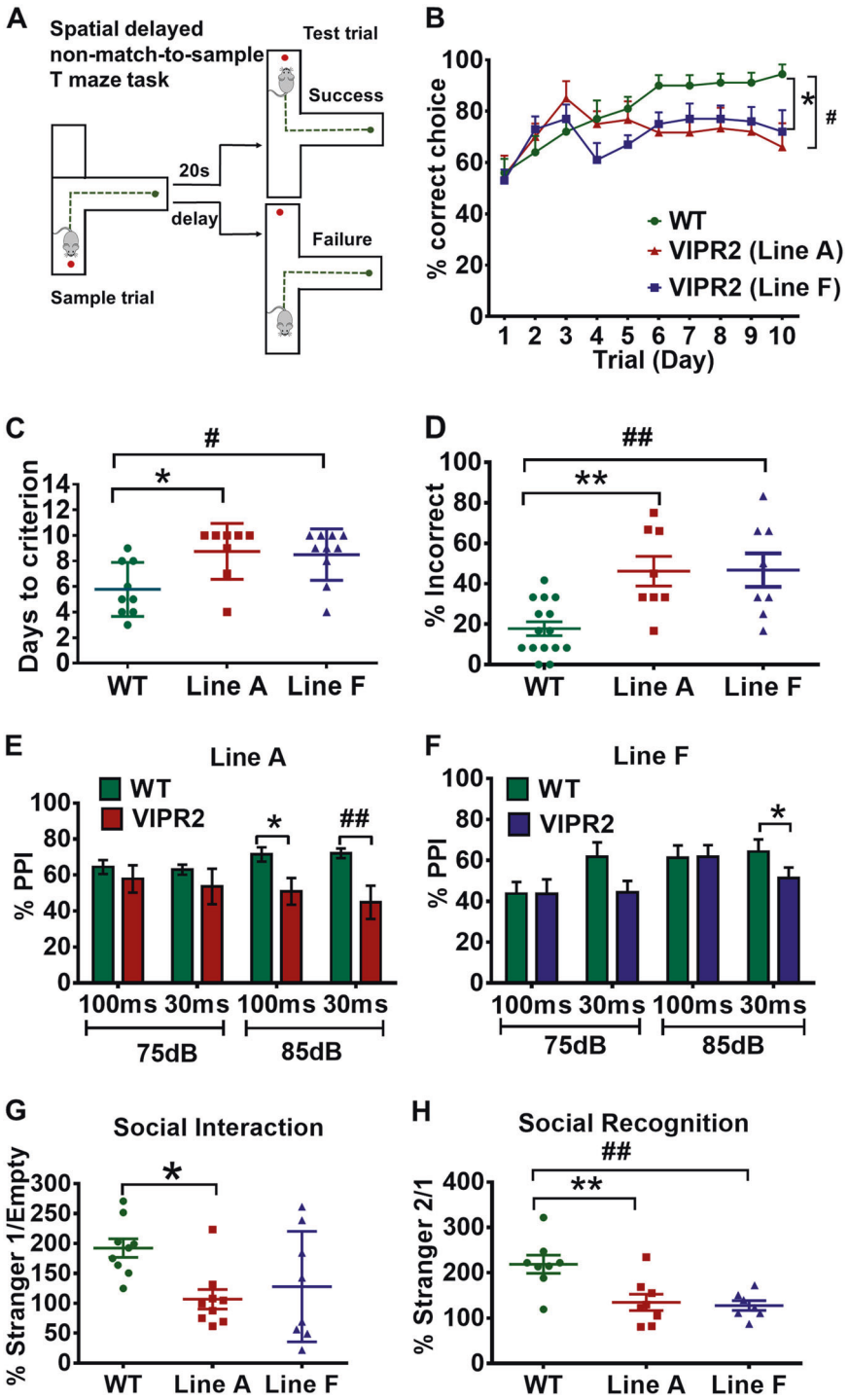

(prepulse) inhibited the reaction to a subsequent stronger startle stimulus (pulse). PPI was indexed by percent inhibition and defined as the percent reduction in reactivity in prepulse-plus-pulse trials relative to pulse-alone trials (Fig. 2e, f). Increasing prepulse intensity led to an increased magnitude of PPI. However, the PPI was significantly reduced in both VIPR2 CNV transgenic lines (A and F) as shown for 85 dB prepulse with 30 ms interstimulus intervals in Line F and 85 dB prepulse with 30 ms or 100 ms intervals in Line A (Student's t test, $*p < 0.05$. For Line A: wildtype: $n = 10$ mice; male: $n = 6$; female: $n = 4$; Line A: $n = 8$ mice; male: $n = 3$; female: $n = 5$; For Line F, wildtype: $n = 7$ mice; male: $n = 3$; female: $n = 4$; Line F: $n = 10$ mice; male: $n = 5$; female: $n = 5$). No changes of startle amplitude or short-term habitation were found in both lines of VIPR2 CNV mice (Supplementary Fig. S6A, B, startle: $F(58,$

◀ **Fig. 2** Schizophrenia-like cognitive and social behavioral deficits in VIPR2 CNV mice. **a** Spatial delayed non-match-to-sample T- maze task. **b** Spatial delayed non-match-to-sample T-maze task data of the percentage of correct responses are represented as means with standard errors and were analyzed by a two-way repeated measures ANOVA (interaction effect: $^{*}p < 0.05$ (Line A); $^{\#}p < 0.05$ (Line F). **c** Acquisition (days to criterion) as a function of genotype and treatment is shown. ($^{*}p < 0.05$ (Line A), $^{\#}p < 0.05$ (Line F). One-way ANOVA, with Turkey's post hoc test. **d** Spontaneous alteration task in T-maze. VIPR2 CNV mice lines (A and F) showed significantly less spontaneous alterations than control mice ($^{**}p < 0.01$ (Line A), $^{\#\#}p < 0.01$ (Line F), one-way ANOVA, with Turkey's post hoc test. **e**, **f** Prepulse inhibition (PPI) of the acoustic startle response deficits in VIPR2 CNV mice. PPI Data (mean ± SEM) shows the percent of prepulse inhibition of the startle response following the presentation of prepulse-plus-pulse acoustic stimuli. Two different interstimulus interval (ISIs) (30 and 100 ms) and two different prepulse intensities (75 and 85 dB) were measured. VIPR2 CNV (Line A) mice showed a significant PPI deficiency when presented with an 85-dB prepulse with 30 or 100 ms ISI (*t*-test; $^{*}p < 0.05$. $^{\#\#}p < 0.01$, while Line F mice have a significant PPI deficiency when presented with an 85-dB prepulse with 30 ms ISI (*t*-test; $^{*}p < 0.05$. **g**, **h** Social approach and social recognition deficits in VIPR2 CNV mice. In the social interaction test, Line A, but not Line F, of VIPR2 CNV mice spent less time in the chamber containing the social partner (Stranger 1), and more time in the chamber containing the empty wire cage when compared with controls ($^{**}p < 0.01$, one-way ANOVA, with Turkey's post hoc test. **h** In the social recognition test, where the mice had a free choice between the first, already-investigated mouse (Stranger 1), and a novel unfamiliar mouse (Stranger 2). Both lines of VIPR2 CNV mice do not display a preference for the novel social partner (Stranger 2). ($^{**}p < 0.01$ (Line A), $^{\#\#}p < 0.01$ (Line F), one-way ANOVA, with Turkey's post hoc test

1044) = 1.265, $p = 0.0917$ for interaction effect, $F(2, 36) = 0.1843$, $p = 0.8325$ for genotype difference).

Impaired social interaction and recognition in a three-chambered social interaction task

We next tested the social function of the VIPR2 CNV mice in a three-chambered apparatus following the standard protocol [40]. The three-chambered task consisted of two trials: social interaction (trial 1) and social recognition (trial 2). In trial 1, we measured the social approach of a mouse toward a stranger mouse trapped in a wire cage versus the approach of an empty wire cage. Next, we evaluated social recognition by allowing mice to have a free choice between the first, already-investigated, familiar mouse (Stranger 1), and a novel unfamiliar mouse (Stranger 2). As shown in Fig. 2g, h, Line A, but not Line F, of VIPR2 CNV mice showed significantly reduced preference for exploring a stranger mouse relative to empty cage compared with wild-type mice as determined by the amount of time spent in each chamber or sniffing cages and the preference index derived from these parameters (Fig. 2g, one-way ANOVA, $F(2,23) = 4.268$, $p = 0.0265$; Turkey's post hoc test, Line A: $p < 0.05$; Line A: $p > 0.05$. Wildtype: $n = 9$ mice; male: $n = 4$; female: $n = 5$; Line A: $n = 9$ mice; male: $n = 5$; female: $n = 4$; Line F: $n = 8$ mice; male: $n = 4$; female: $n = 4$). In the social recognition test, both lines of VIPR2 CNV mutants showed a significantly impaired preference for the chamber containing a newly introduced mouse (Stranger 2) over a chamber containing a now-familiar mouse (Stranger 1, Fig. 2h, one-way ANOVA, $F(2,20) = 8.773$, $p = 0.0018$; Turkey's post hoc test, Line A: $^{**}p < 0.01$; Line A: $^{**}p > 0.01$. Wildtype: $n = 8$ mice; male: $n = 5$; female: $n = 3$; Line A: $n = 8$ mice; male: $n = 3$; female: $n = 5$; Line F: $n = 9$ mice; male: $n = 5$; female: $n = 4$), indicating an impairment of social recognition memory. Also, in one of the lines of the VIPR2 CNV mice (Line F), we observed nest building deficits (Supplementary Fig. S7A–C), suggesting social function deficits in VIPR2 CNV mice. The two independent founder lines were characterized in detail in order to exclude the positional effects due to the disruption of genomic loci by random integration since it is highly unlikely that two independent transgenic insertions occur at the same locus [41, 42]. Therefore, in the following pathology studies, we focused our analysis on Line A with the human VIPR2 duplication.

Prominent dorsostriatal DA neurotransmission abnormalities in VIPR2 CNV mice

It has been suggested that excess DA neural transmission through DA type 2 receptors (D2r) in the striatum is an underlying mechanism of schizophrenia pathogenesis [24]. D2r immunostaining was performed in the VIPR2 CNV mice and wild-type littermates at 3–5 months of age using an antibody widely used and validated in the KO mice (Millipore AB5084P) [43]. The D2r immunostaining was contoured and quantified using the Image J in each of the subregions of the striatum as previously described [44] and depicted in Supplementary Fig. S1A: the dorsolateral, dorsomedial, and ventral striatum that approximately correspond to three functional domains: the sensorimotor, associative, and limbic domains, respectively. The immunostaining of the D2rs was consistently found increased in the dorsal subregions of the striatum, but not in the ventral subregions of the striatum in both founder lines of the VIPR2 CNV mice compared with WT mice (Line F, Fig. 3a–c. Figure 5f, g for Line A, and Supplementary Fig. S8A–D for Line A shown in both sagittal (C, D) and coronal sections (A, B). VIPR2 CNV mice have an about 20% of increase of D2r in the dorsal striatum, which is comparable to D2r abnormalities observed in human neuroimaging study [45]. We also observed an increase of the dopaminergic terminal input to dorsal striatum as immunostained by tyrosine hydroxylase (TH) antibody (Line A, Fig. 3e–g, $n = 4$ per genotype). The DA D1 receptor expression in the dorsal striatum (Supplementary Fig. S8E, F, Line A) was also increased as evaluated by the GFP staining in the Drd1a-GFP/VIPR2 CNV double

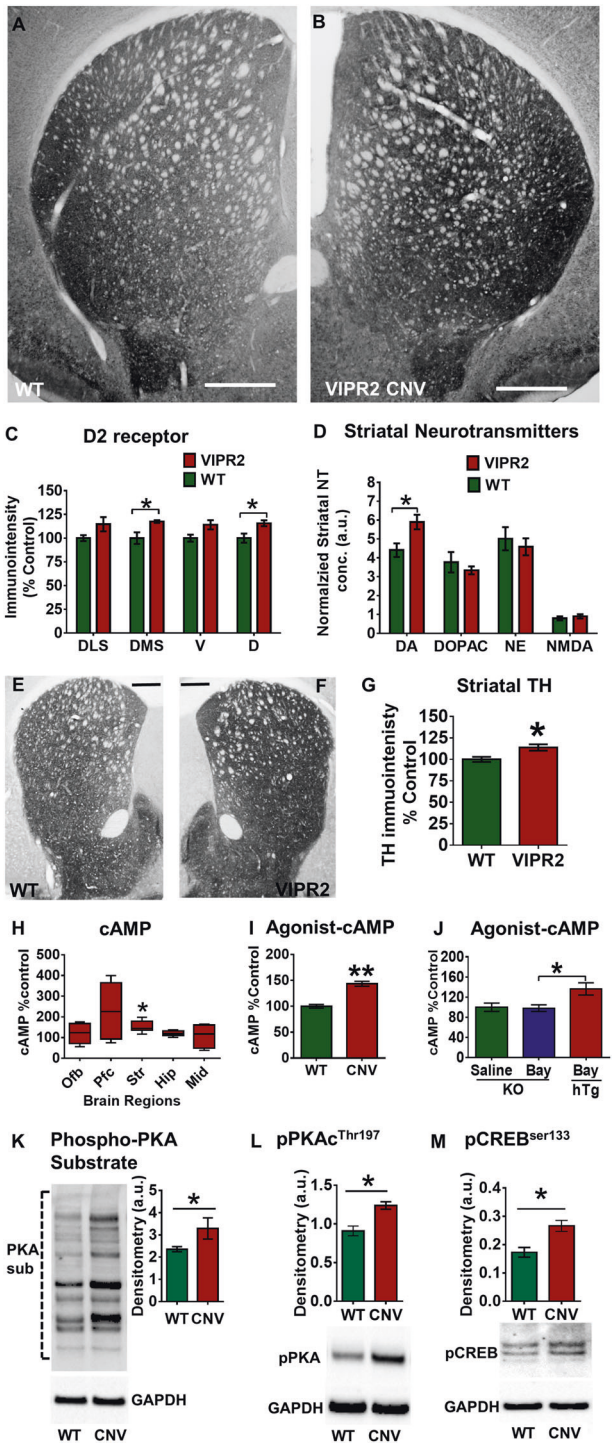

◀ **Fig. 3** VIPR2 CNV elicited striatal dopamine neural transmission and cAMP/PKA signaling deficits in mice. **a**-**c** Both founder lines of VIPR2 CNV mice (shown images of Line F) at 3 months of age had an increase D2 receptor immunostaining in dorsomedial (DMS, associative, A), dorsolateral (DLS, sensorimotor, S), and dorsal striatum (d), but not in the ventral striatum (V). Scale bar = 500 µm. **c** Quantification of the D2r immunostaining intensity in different subregions of the striatum revealed that VIPR2 CNV mice (Line F) have a significant increase of D2r in the DMS and whole dorsal striatum (both rostral and caudal levels of coronal sections were used for quantification. The data were expressed as the average of both left and right hemisphere immunostaining intensity. $n = 4$ mice per genotype, t-test, $^*p < 0.05$). **d** Dorsostriatal dopamine content was significantly increased in the VIPR2 CNV mice (Line A) at 3 months of age as measured by HPLC ($^*p < 0.05$, t-test, $n = 6$ per genotype) in the VIPR2 CNV mice. **e**–**g** VIPR2 CNV mice (Line A) had an increase of TH immunostaining in the dorsal striatum ($^*p < 0.05$, $n = 4$ per genotype, scale bar = 500 µm). **h** VIPR2 CNV mice (Line A, postnatal day 18, P18) showed an increased striatal cAMP level (pmol cAMP/mg protein expressed as a percentage of control mice) in the striatum. No significant difference of cAMP levels was observed in the olfactory bulb (Ofb), hippocampus (Hip), and midbrain (Mid) (one sample t-test; $^*p < 0.05$, $n = 8$ per genotype). **i** Adult VIPR2 CNV mice (Line A, 3–5 months old) have significantly elevated cAMP accumulation in both cortex and striatum 1 h after intraperitoneal injection (i.p.) of a selective VIPR2 agonist, BAY 55–9837 (0.25 µg/g), $^{**}p < 0.01$, $n = 4$ mice per genotype/treatment. **j** The accumulation of cAMP in the humanized mouse model and VIPR2 knockout mouse model after BAY 55–9837 (0.25 µg/g) i.p. ($^*p < 0.05$, $n = 4$ mice per genotype/treatment, 3–5 months). **k** p(Ser/Thr) PKA substrates levels were analyzed by western blot of the striatum from WT and VIPR2 CNV mice at P18. **l** pPKAcThr197 and **m** PKA-dependent phosphorylation of CREBser133 were analyzed by western blot of protein extracts obtained from the striatum of WT and VIPR2 CNV mice (P18). For p(Ser/Thr) PKA substrates, all the bands were used for quantification (t-test; $^*p < 0.05$, $n = 4$ or 5 mice per genotype)

transgenic mice. Finally, tissue monoamine levels were measured in the dorsal striatum of the VIPR2 CNV mice by HPLC. The main finding was a significant increase of DA (Fig. 3d, Line A, t-test, $p < 0.05$, $n = 6$–8 per genotype), but not 3,4-dihydroxyphenylacetic acid, 5-hydroxytryptamine, and norepinephrine levels in the dorsal striatum (Fig. 3d, Line A, t-test, $p > 0.05$, $n = 6$–8 per genotype). All these results collectively suggest that VIPR2 CNV mice have a prominent dorsostriatal DA neurotransmission abnormality.

Abnormally increased cAMP/PKA signaling in VIPR2 CNV mice

Since VIPR2 is a stimulatory Gs-GPCR, we quantified baseline cAMP levels in different brain regions of VIPR2 CNV mice and control mice in adult mice and the early postnatal stage at P18. We did not detect a significant baseline cAMP level change in adult mice. However, the cAMP levels were significantly increased (pmol cAMP/mg protein expressed as a percentage of control mice) in the striatum (Fig. 3h) of VIPR2 CNV mice (Line A) at P18. Phosphorylation of Thr197 in the activation loop of the catalytic subunit of PKA (PKAc) is an essential step for its proper biological function. Thus, to further explore the increased activation of PKA during development, we analyzed the levels of pPKAcThr197 in VIPR2 CNV (Line A) and wild-type mice by western blot at P18. We observed a significant increase in the levels of pPKAcThr197 in the striatum of VIPR2 CNV mice

compared with their littermate controls (Fig. 3l). PKA activity was further evaluated by using an antibody (Cell Signaling Technology, #9621) that detects its serine/threonine substrates when phosphorylated at the PKA consensus region (Fig. 3k). Finally, PKA-dependent phosphorylation of CREBser133 was increased in VIPR2 CNV mice (Fig. 3m) at P18. In summary, we found that the basal cAMP/PKA activity was increased in the striatum of the VIPR2 CNV mice, which suggests that VIPR2 overexpression increases the constitutive activity of the receptor acting by endogenous ligands, e.g., VIP or PACAP.

To further explore the striatal cAMP deficits in adult mice and to confirm the human VIPR2 transgenes are functional, we examined the effects of a selective VPAC2 agonist (BAY 55–9837, 0.25 µg/g intraperitoneal injection (i.p.) 1 h before killing) to stimulate brain cAMP level in adult VIPR2 CNV and wild-type mice (3–5 months of age). Peripheral administration of VIP and PACAP receptor agonists have been shown to have behavioral and neurobiological effects [46]. Importantly, early postnatal administration of a VPAC2 agonist elicits profound neurodevelopmental changes, including synaptogenesis and PPI deficits in mice [13]. To confirm that BAY 55–9837 has a good blood–brain-barrier penetration after acute i.p. delivery, we used a mouse line of luciferase reporter of cAMP/cAMP response element binding protein (CREB) activity [47] to monitor VPAC2 agonist-stimulated CREB activity in vivo. BAY 55–9837, 0.25 µg/g i.p. stimulated CREB activity in the full body rapidly and significantly increased the brain CREB activity 1 h after i.p. injection (Supplementary Fig. S9A, B, $n = 3$). In adult mice, BAY 55–9837, 0.25 µg/g i.p also significantly increased the striatal cAMP level in VIPR2 CNV Mice (Line A) in comparison to control littermates (Fig. 3i). In the human study, VIPR2 agonist BAY 55–9837 (100 nM) stimulated a 30% increase in cAMP signaling in lymphoid cell lines derived from patients with VIPR2 microduplication, which is consistent with what we observed in the striatum in the adult mice [7].

In order to confirm the specificity of the BAY 55–9837 on the human VIPR2 receptor, we further measured the accumulation of cAMP in the humanized mouse model and VIPR2 knockout mouse model. BAY 55–9837 did not induce cAMP accumulation in the KO mice but significantly increased cAMP accumulation in the humanized VIPR2 transgenic mouse model in the striatum (Fig. 3j, $p < 0.05$, $n = 4$ mice per genotype/treatment). All these data convincingly demonstrated that adult VIPR2 CNV mice have a striatal cAMP/PKA signaling abnormality. Furthermore, human VIPR2 is overexpressed in the transgenic mice and is functional in transducing the extracellular stimuli into intracellular signals.

Striatal developmental deficits in VIPR2 CNV mice

Given the robust role of VIP signaling in striatal neurons, our observation of the early postnatal cAMP/PKA signaling deficit suggests that VIPR2 CNV may disrupt the striatal development to manifest adult DA and behavioral deficits. During early postnatal development of striatal circuitry, rapid excitatory spinogenesis usually lasts from P8 to P18 in mice [26] and significantly contributes to efficient striatal circuit wiring. Indeed, VIPR2 is expressed in the striatum at this critical period, starting from postnatal day 4 (P4), as characterized by the Allen Brain Institute (Supplementary Fig. S10A–C). VIPR2 gene expression is limited to SPNs in the striatum and the layer 3–5 pyramidal projection neurons in the cortex and hippocampus, with very low-level expression at SCN.

In order to assess the potential pathogenic role of VIPR2 CNV on early postnatal striatal development, we focused our analyses on striatal SPNs and expiatory synaptic inputs to the striatum. First, to confirm the findings on altered synaptic protein levels, we performed IHC staining and western blot using striatum of mice at the 2nd week of postnatal development. Vesicular glutamate transporters (VGLUTs) located in the membrane of presynaptic glutamatergic vesicles are responsible for loading glutamate into the vesicles before they release their content into the synaptic cleft by fusing with the presynaptic membrane (exocytosis). Since the number of VGLUT molecules per synaptic vesicle has a major impact on the quantal size in glutamatergic neurons, the expression levels of VGLUT protein are an indication for the relative synaptic strength of presynaptic glutamatergic innervation for a given brain region [48].

In VIPR2 CNV mice (Line A), we observed a significant increase in the intensity of VGLUT1 immunostaining (Fig. 4a–d, e) and VGLUT1 protein levels (Fig. 4e, f, *t*-test, $p < 0.05$) in the striatum of the VIPR2 CNV mice in comparison to the wild-type mice. At P8 striatum, VIPR2 CNV mice also have significantly increased VGLUT2 immunostaining, which is a marker for thalamic excitatory inputs (Supplementary Fig. S10E, *t*-test, $p < 0.05$, $n = 4$ per genotype). We found the presynaptic marker synaptophysin level was also significantly increased in the striatum (western blot, data not shown). All these results collectively indicate that striatal SPNs in VIPR2 CNV mice received abnormally increased excitatory inputs in comparison to wild-type littermates during early postnatal development.

Interestingly, we have found VIPR2 expressed in a patch-like structure in the striatum at P8 (Supplementary Fig. S10D). During the 2nd week of postnatal striatal development, the major afferents to the striatum, such as the cortical and thalamic glutamatergic afferents, delineates a patch-like organization to form “afferent islands” in the

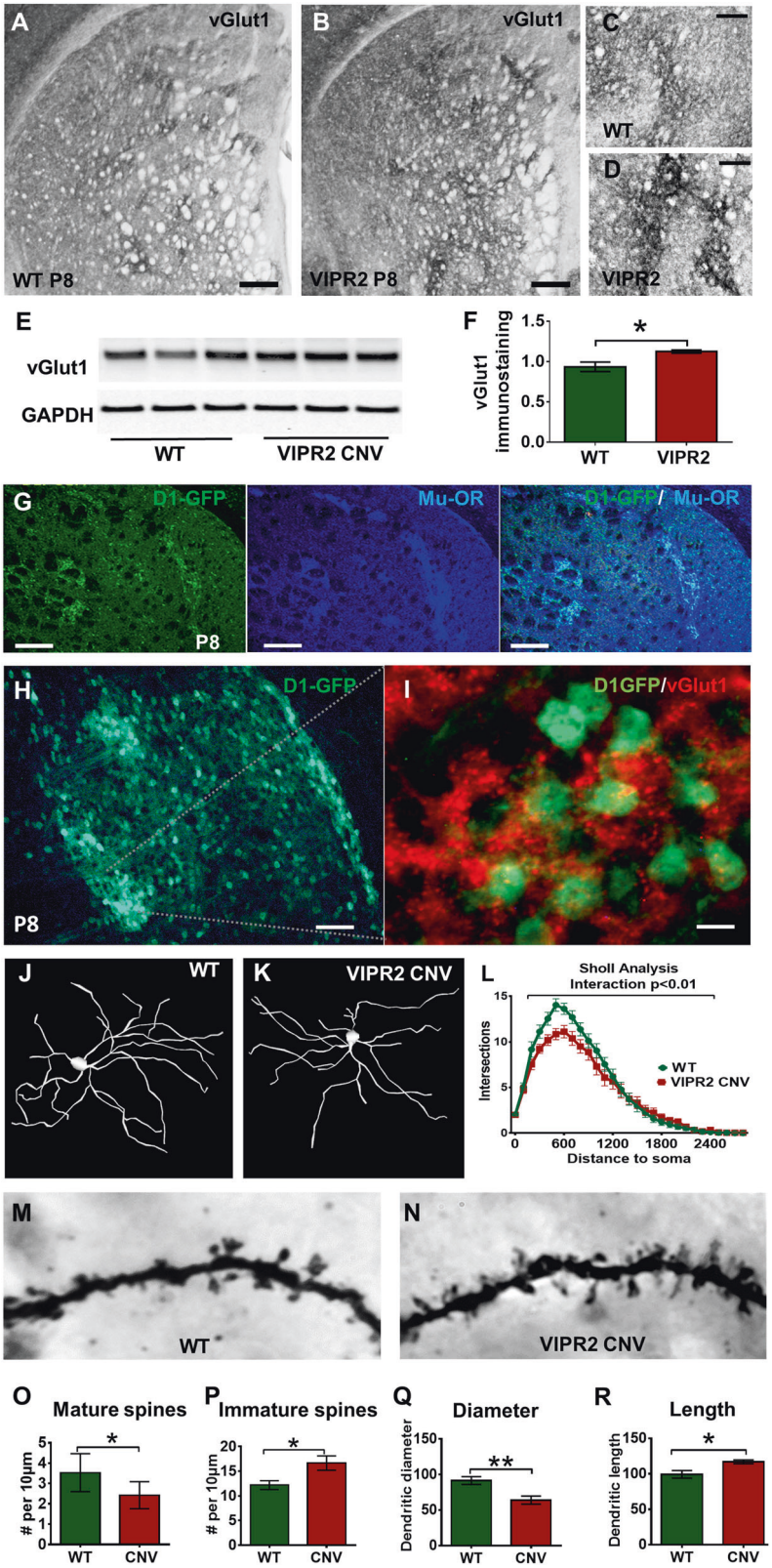

immature striatum [49]. Others and our data [50] using the GENSAT Drd1a-BAC-GFP mice have consistently found that D1 receptor-expressing dSPNs are preferentially localized within the afferent islands. As shown in Fig. 4g–i, the localization of dSPN patches corresponded to striosomes identified by mu opioid receptor (MuOR) staining

◀ **Fig. 4** Early postnatal striatal developmental pathology in the VIPR2 CNV mice. **a–b** At P8, VGLUT1 immunostaining delineates a patch-like "afferent islands" in immature striatum. Scale bar = 100 µm. **c–d** Higher magnification of striatum in wild-type and VIPR2 CNV mice (Line A). Scale bar = 25 µm. **e** VGLUT1 protein levels in the striatum in VIPR2 CNV mice (Line A) are significantly increased in comparison to that of the wild-type mice ($n = 3$ per genotype, t-test, $^{*}p \leq 0.05$). **g** In the Drd1a-GFP BAC mice at P8, the localization of dSPNs patches (GFP staining, green) corresponded to striosomes identified by mu opioid receptor (MuOR) staining (blue). Scale bar = 100 µm. **h–i** dSPN patches colocalize with the intense VGLUT1 immunoreactivities as revealed by double immunofluorescence labeling for VGLUT1 (red) and dSPNs (green) at P8. Scale bar = 50 µm. Multiple brains from wild-type littermates and VIPR2 CNV mice at P18 were subjected to Golgi staining. **j–k** Representative traces of SPNs in wild-type littermates and VIPR2 CNV mice. **l** Sholl analysis of intersection of SPNs in VIPR2 CNV mice and wild-type littermates (30 neurons from six mice per genotype) identified a significant genotype–distance interaction ($p < 0.01$, repeated measure two-way ANOVA. **m**, **n** Representative high magnification images of dendritic spines of SPNs from wild-type littermates and VIPR2 CNV mice. **o–r** Dendritic spines of SPNs were categorized in immature (thin and filopodia-like) or mature spines (mushroom, stubby, and multiple spine post synapses). **o** An average number of mature spines (mushroom) per 10 µm dendritic length in SPNs from VIPR2 CNV mice (Line A) is significantly lower than that of wild-type SPNs (t-test; $^{*}p < 0.05$). **p** An average number of immature (thin) spines per 10 µm dendritic length in SPNs from VIPR2 CNV mice is significantly higher than that of wild-type SPNs (t-test; $^{*}p < 0.05$). **q** The diameter of the dendrites in SPNs from VIPR2 CNV mice is significantly lower than that of wild-type SPNs (t-test; $^{**}p < 0.01$). **r** The average length of spines in SPNs from VIPR2 CNV mice is significantly longer than that of wild-type SPNs (t-test; $^{*}p < 0.05$)

and VGLUT1 staining. The striosomal pattern of dSPNs disappears and becomes progressively uniform in the whole striatum due to the increase of the dSPNs in the matrix during the third postnatal week [51]. Our recent study using single-neuron transgenic strategy to visualize the dendritic development of dSPNs [50] also revealed drastic dendritic maturation in the 2nd postnatal week. During this critical period, corticostriatal connectivity has been reported to be highly sensitive to changes in striatal neuromodulation [26].

Finally, to test whether VIPR2 CNV affects dendritic morphology of the striatal SPNs, we performed Golgi staining in wild-type and VIPR2 CNV mice (Line A) at P18, using the FD Rapid GolgiStain™ Kit (FD NeuroTechnologies, Columbia, MD). We traced Golgi-stained striatal SPNs and their dendrites to investigate the cellular morphology and complexity of these cells (Fig. 4j–n). Sholl analysis revealed a dendritic hypertrophy as measured by a significant decrease in the complexity of dendritic arborization in VIPR2 CNV SPNs (Fig. 4l, two-way ANOVA with repeated measure by genotype, $F(28, 1624) = 2.561$, $p < 0.01$ for interaction of genotype with distance to soma; $F(1, 58) = 1.240$, $p = 0.1291$ for genotype, $n = 30$ neurons per genotype from six mice). We next categorized the dendritic spines based on their morphologies and found that there was a significant alteration between the genotypes (Fig. 4o–r, t-test, $^{*}p < 0.05$). An increased number of immature spines (thin and filopodia-like, 4P, t-test, $^{*}p < 0.05$) and spine length (4R, t-test, $^{*}p < 0.05$), but significantly reduced mature spines (4O, t-test, $^{*}p < 0.05$), and dendritic diameters (4Q, t-test, $^{**}p < 0.01$) were seen in VIPR2 CNV mice. In summary, these results suggest that striatal SPNs received abnormal glutamatergic innervation and the early postnatal striatal dendritic development was disrupted in the VIPR2 CNV mice.

Genetic removal of VIPR2 transgene expression in D1 receptor-expressing neurons rescued the D2 receptor abnormality and multiple behavioral deficits in VIPR2 CNV mice

It has been established that striatal dSPNs (expressing D1 receptor as a marker) play a biased "driver" role in early postnatal striatal neurodevelopment [26]. Furthermore, D1 receptor-expressing neurons in striatum and cortex are of critical importance in cognitive function and behavioral manifestation of schizophrenia [52, 53]. Our VIPR2 CNV mice were generated using conditional BAC transgenesis where the first exon of VIPR2 with the endogenous translation initiation codon was floxed by two loxP sites. Therefore, the overexpression of VIPR2 could be switched off in desired temporal and spatial patterns controlled by crossing with mice expressing Cre recombinase (Fig. 5a). Employing the conditional BAC transgenesis, we first set out to address if VIPR2 transgene expression in D1 receptor-expressing neurons plays a causal pathogenic role in the manifestation of schizophrenia-like DA and behavioral deficits.

We crossed the VIPR2 CNV mice with GENSAT Drd1a-Cre BAC transgenic mice that express Cre recombinase driven by the endogenous mouse D1r promoter. Using the tdTomato reporter mice (Ai9) [54], we have confirmed the expression of the Cre recombinase expression pattern (Fig. 5b). Therefore, the VIPR2 transgene expression could be removed in D1 receptor-expressing neurons during neural development and in adult mice. We confirmed the reduced VIPR2 gene expression in striatum and cortex using qRT-PCR (Fig. 5e, t-test, $^{*}p < 0.05$; $^{\#\#}p < 0.01$, $n = 4$ per genotype). We also found significantly reduced immunopositive cells and staining intensities via IHC staining of human VPAC2 in the striatum (Fig. 5c, d). Importantly, selective removal of VIPR2 transgene expression in D1 neurons rescued striatal D2 receptor overexpression abnormality (Fig. 5f, g, one-way ANOVA, $F(2, 9) = 17.21$, $p = 0.0008$, with Tukey's post hoc test, $^{**}p < 0.01$; $^{\#}p < 0.05$, $n = 4$ per genotype), spatial working memory impairment in T-maze (Fig. 5h, one-way ANOVA, $F(2,37) = 14.53$, with Turkey's post hoc test; $^{*}p < 0.05$, $^{\#\#}p < 0.01$, control group includes wildtype and D1-Cre littermates, $n = 17$ mice; wildtype: $n = 10$; D1-Cre: $n = 7$;

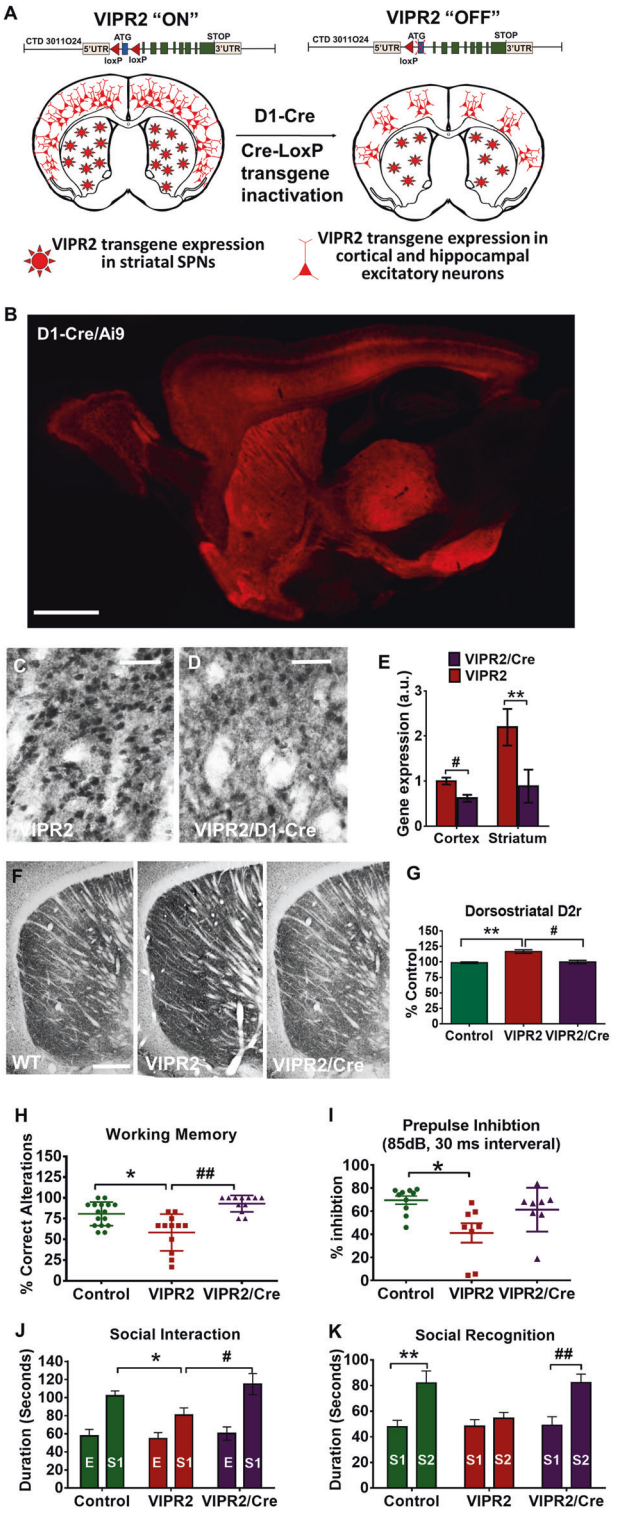

Fig. 5 Genetic removal of VIPR2 CNV in D1r-expressing neurons rescues dopamine and cognitive deficits in VIPR2 CNV mice. **a** Schematics of the conditional BAC transgenesis to remove human VIPR2 transgene expression in D1r-expressing cells via crossing with Drd1a-BAC-Cre (D1-Cre) mice. **b** Epifluorescence imaging D1-Cre recombinase activity in the D1-Cre mice crossing with a reporter mouse line (Ai9). Scale bar = 500 µm. **c**, **d** Reduced the number of VPAC2 immunopositive cells in the striatum of the VIPR2 (Line A)/D1-Cre double transgenic mice. Scale bar = 50 µm. **e** Significantly reduced VIPR2 expression in the cortex and striatum of the VIPR2 (Line A)/D1-Cre double transgenic mice quantified by qRT-PCR (*t*-test; $^{**}p < 0.01$, $^{\#}p < 0.05$). **f** Dorsostriatal D2 receptor overexpression abnormality as revealed by IHC was rescued in the VIPR2 (Line A)/D1-Cre double transgenic mice at 3–5 months of age (scale bar = 100 µm). **g** The contour of the dorsal striatum and quantification of the staining intensity (one-way ANOVA, with Turkey's post hoc test; $^{**}p < 0.01$, control in comparison to VIPR2 CNV (Line A); $^{\#}p < 0.05$, VIPR2/Cre in comparison to VIPR2 CNV (Line A). **h** Working memory deficit (spontaneous alteration in T-maze) in the VIPR2 CNV mice (Line A) were rescued (one-way ANOVA, with Turkey's post hoc test; $^{*}p < 0.05$, $^{\#\#}p < 0.01$. **i** Genetic removal of VIPR2 CNV in D1r-expressing neurons rescues PPI deficit in VIPR2 CNV mice (Line A) shown at 85 dB, 30 ms interval (one-way ANOVA, with Turkey's post hoc test; $^{*}p < 0.05$, $^{\#}p < 0.05$). Genetic removal of VIPR2 CNV in D1r-expressing neurons rescues social interaction (**j**) and recognition (**k**) deficits in VIPR2 CNV mice (Line A, 3–5 months of age, data are expressed as the duration (seconds) of mice to contact with stranger mouse or empty cage, one-way ANOVA, with Turkey's post hoc test; $^{*,\#}p < 0.05$, $^{**,\#\#}p < 0.01$. E empty cage, S1 stranger 1, S2 stranger 2)

male: $n = 9$; female: $n = 8$ mice; VIPR2 group: $n = 12$ mice, male: $n = 5$; female: $n = 7$ mice; VIPR2/D1-Cre group: $n = 12$ mice, male: $n = 5$; female: $n = 7$ mice), and sensorimotor gating deficit (Fig. 5i, one-way ANOVA, $F(2, 23) = 5.584$, $p = 0.0106$, with Turkey's post hoc test; $^{*}p < 0.05$. Control group includes wild-type and D1-Cre mice. Control: $n = 10$; wildtype: $n = 6$; D1-Cre: $n = 4$; male: $n = 5$; female: $n = 4$ mice; VIPR2 group: $n = 8$ mice; male: $n = 5$; female: $n = 3$ mice; VIPR2/D1-Cre group: $n = 8$ mice, male: $n = 4$; female: $n = 4$ mice). Finally, genetic removal of VIPR2 CNV in D1r-expressing neurons rescues social interaction (5 J) and recognition (5 K) deficit in VIPR2 CNV mice (Fig. 5j, k, Line A, 3–5 months of age) (one-way ANOVA, social interaction: $F(2,23) = 5.584$, $p = 0.0106$; social recognition: $F(2,25) = 3.384$, $p = 0.0353$, with Turkey's post hoc test; $^{*}p < 0.05$. $^{\#}p < 0.05$. $^{\#\#}p < 0.01$. Control group includes wild-type and D1-Cre mice. Control: $n = 14$; wildtype: $n = 9$; D1-Cre: $n = 5$; male: $n = 6$; female: $n = 8$ mice; VIPR2 group: $n = 11$ mice; male: $n = 5$; female: $n = 6$ mice; VIPR2/D1-Cre group: $n = 10$ mice, male: $n = 4$; female: $n = 6$ mice). In all these behavioral tests, we have determined that D1-Cre mice do not have significant behavioral deficits in comparison to wild-type mice (Supplementary Fig. S11A–D). Therefore, the control group included both the wild-type and D1-Cre mice. The genetic dissection results collectively suggest that remove the VIPR2 overexpression in dopaminoceptive neurons can rescue the D2 receptor abnormality and multiple behavioral deficits in VIPR2 CNV mice. Taken together, we have provided further evidence to support the GWAS studies that the dosage sensitivity intolerance of VIPR2 is causative in the manifestation of schizophrenia-like DA neurotransmission, cognitive, and social, behavioral deficits as summarized in the Supplementary Table S1.

Discussion

Dosage sensitivity intolerance of VIPR2 CNV is disease causative

The convincing association of some CNVs with neurodevelopmental disorders poses intriguing questions about their pathogenic roles. It has been hypothesized that dosage sensitivity is a major determinant of human CNV pathogenicity. The pathogenic CNVs are usually enriched for genes with high evolutionary copy constraints and involved in developmental processes [3]. In the GWAS study [7], all of the VIPR2 microduplications (three copies) and triplications (four copies) of human chromosomal region 7q36.3 lie within VIPR2 genomic locus or the gene-less subtelomeric region < 89 kb from the transcriptional start site [7]. Mouse VIPR2 is in the telomeric region of chromosome 12, which is syntenic to human chromosomal region 7q36.3. The VIPR2 transcripts detected by sequencing in patients with duplications are the normal size, suggesting a tandem repeat. The duplications and triplications of 7q36.3 result in increased VIPR2 transcription and cyclic-AMP signaling. In lymphoid cell lines derived from patients with 7q36.3 duplication and triplications, VIPR2 transcription is increased by twofold and cAMP responses to VIP and VIPR2 selective agonist BAY 55–9837 were significantly increased by 30% as compared with controls [7]. These findings implicated a pathogenic role of increased VIPR2 gene dosage, expression, and its downstream signaling in schizophrenia, but with a defined level of confidence for disease causality.

In order to provide further evidence to support the disease causality of the VIPR2 duplication, we generated a series of conditional VIPR2 BAC transgenic mouse models of VIPR2 CNV. We observed consistent behavioral and DA deficits in two independent BAC lines, with no obvious gene dosage effects. The two independent founder lines were characterized in detail in order to exclude the positional effects due to the disruption of the genomic locus by the random integration since it is highly unlikely that two independent transgenic insertions occur at the same locus [42].

VIPR2 CNV mouse model recapitulates the gene expression and signaling deficits seen in human CNV carriers. VIPR2 duplication in mice elicits prominent dorsal striatal DA dysfunction. Young adult VIPR2 CNV mice manifest cognitive, sensorimotor gating, and social behavioral deficits that preceded by an increase of striatal cAMP/PKA signaling, striatal neuron dendritic deficits, and disrupted early postnatal striatal development. Remove of the transgene overexpression can rescue the DA and behavioral symptoms. As shown in Supplemental Table 1, the similarities between symptoms of schizophrenia and the alterations elicited in VIPR2 CNV BAC transgenic mice are consistent with the GWAS studies and suggest that increased VIPR2 expression or intracellular cAMP/PKA signaling may play a key role in the pathogenesis of schizophrenia.

Furthermore, VIPR2 duplication was also highly represented in ASD in one of the GWAS studies [7]. The ligand of the VPAC2 receptor, VIP, has been found nearly tripled the normal level in the blood of neonates with ASD [55]. VIPR2 CNV mice manifested ASD-like traits with disruption of social, cognitive, and striatal neurodevelopment. Once considered the same disorder expressed in different developmental periods, ASD and schizophrenia are both neurodevelopmental disorders characterized by similar social and cognitive deficits and with shared genetic and neurobiological mechanisms, suggesting etiological commonality [56]. Intriguingly, Stefansson et al. demonstrated that even phenotypically healthy carriers of CNVs have cognitive deficits [57]. Therefore, the pathogenic role of the VIPR2 duplication could be pleiotropic and can give rise to many different neuropsychiatric phenotypes that are on a developmental continuum.

VIPR2 CNV is a rare variant that can substantially increase schizophrenia risk. Different from the common variants associated with small disease risk, rare variants usually cause nonsynonymous or gene dosage changes [58]. Therefore, rare variants offer a better opportunity to facilitate the development of animal models to assess the impact of the genetic vulnerability on brain development and behavioral manifestations. The strategy to introduce a human allele in mouse models has been extensively employed to unravel the causality and pathogenic mechanisms of CNVs. Different from the conventional transgenic or conditional knockout approaches, here we described a conditional BAC transgenic strategy [59] to model the neurodevelopmental CNV and to dissect the inflicted neurocircuits. Taking into consideration that the average mammalian transcriptional unit is about 25 kb, the 231-kb human BAC we modified encompasses the complete set of *cis*-transcriptional regulatory elements to direct the human VIPR2 gene expression. The sheer size of the BAC renders the expression of the transgene to be buffered from the influence of enhancers and repressors surrounding the integration site, so as to avoid the positional effects that plagued conventional transgenesis [42]. Therefore, BAC approach can faithfully reproduce endogenous human VIPR2 transgene expression pattern in different brain regions with a better construct and predictive validities. Furthermore, the conditional design to flox the transgene, and the conditional genetic approach will pinpoint the pathogenic role in a genetically defined population of neuronal cell types in different brain regions. Thus conditional BAC transgenesis provides a novel strategy to model CNVs

with a gain-of-copies and to dissect its pathogenic role by linking the candidate genetic vulnerabilities to dysfunctional neuronal subtypes and circuits.

Abnormally elevated VPAC2/PKA signaling disrupts striatal development and connectivity

As all DA receptors are either positively or negatively coupled to an intracellular cAMP/PKA signaling cascade, dysfunction of the second messenger system has been associated with abnormal brain neurodevelopment and schizophrenia [60]. Similar to our observation, Kelly et al. has found an early postnatal increase of striatal cAMP levels, but not in adult mice, in a mouse model overexpressing Gαs G-protein subunit linked to schizophrenia [61]. Revealed from the sophisticated genetic dissections in the study, elevated of Gαs/cAMP signaling only during development was sufficient to manifest adult PPI, spatial learning and memory, and neuroanatomical deficits. Thus, too much or too little intracellular cAMP signaling cascade during development can affect neural circuits and function.

Indeed, we have found early postnatal striatal developmental deficits in VIPR2 CNV mice that manifested as the elevated cAMP/PKA signaling, increased striatal excitatory inputs, and striatal dendritic maturation deficit. Impairments of dendritic and synaptic density in the caudate and putamen, such as changes in dendritic arborization, dendritic spine number/type, and morphology, were consistently observed in schizophrenia patients [62]. Future studies need to determine if such dendritic developmental deficits are causal to the adult manifestation of DA receptor abnormality and behavioral phenotypes. To address this question, the inducible Cre system can be employed to delete the overexpression of VIPR2 in the critical striatal developmental stages. Furthermore, it is valuable to examine if medications that can correct the consequences of such developmental deficits could restore normal structure and function of the inflicted neurocircuits.

During early postnatal development of the striatum, the majority of corticostriatal and thalamostriatal synaptogenesis and circuit connections occurs postnatally. SPNs have rapid maturation of excitatory synaptogenesis from P8 to 18 driven by the release of glutamate from axon input from other brain regions [63]. At this period of striatal development, both cortical and thalamic glutamatergic afferents form “afferent islands” in the immature striatum [49]. As shown in Fig. 4g–i, we found such glutamatergic islands overlap with patch-like structures of dSPNs, suggesting that dSPNs undergo very early excitatory synaptogenesis and may play an “anchor” role to consolidate the excitatory inputs, thus critical for the maturation of the whole striatum. Interestingly, early postnatal expression of VIPR2 also demonstrates a patch-like pattern the striatum (Supplementary Fig. S10D).

It has been shown that corticostriatal connectivity is highly sensitive to changes in striatal neuromodulation during early postnatal striatal development [26]. Kozorovitskiy et al. recently revealed a general role of neuromodulation mediated by Gαs GPCR/PKA signaling in SPNs, which is required for both dSPNs and iSPNs to establish excitatory synaptogenesis during early postnatal development. Importantly, during early postnatal development, PKA signaling in dSPNs, but not iSPNs, play a biased driver role to regulate cortical glutamate-dependent circuit wiring via polysynaptic recurrent loops [26].

As shown in the Fig. S1, given the robust role of VIP on cAMP/PKA signaling in the striatum, our results demonstrate that human VIPR2 overexpression in SPNs modulates striatal DA/PKA signaling in derailing the developmental trajectory of the striatal circuit and its connectivity with the cortex, thalamus, and other brain regions. Importantly, the genetic removal of VIPR2 CNV in D1 receptor-expressing cells rescues the DA receptor abnormality and multiple behavioral deficits in VIPR2 CNV mice, thus establishing a causal link that the VIPR2 overexpression in the dopaminoceptive neurons, especially D1 receptor expression neurons, is causative to manifest schizophrenia-like DA and behavioral deficits.

How could a striatal abnormality lead to schizophrenia-like behavioral phenotypes in mice?

In the VIPR2 CNV mice, we found a prominent DA neurotransmission abnormality in the dorsal striatum, consistent with the recent human imaging findings. Largely based on observation of the psychostimulant elicited locomotion, the early DA hypothesis of schizophrenia proposed that the mesolimbic dysfunction underlay positive symptoms. However, recent neuroimaging studies have an unanticipated finding that that DA dysfunction in schizophrenia is the greatest within dorsal striatum [21]. These findings have convincingly pinpointed the associative striatum as the brain region with the greatest differences in DA dysfunction (e.g., increase of DA synthesis and D2 receptor density), with differences in the limbic striatum not reaching statistical significance [64, 65]. Importantly, individuals at high risk of schizophrenia also have the prominent dysfunction in the associative striatum, suggesting striatal DA abnormalities are present prior to the onset of schizophrenia and thus are not a consequence of psychosis episode [22]. It has been proposed that striatal DA abnormality constitutes an endophenotype of schizophrenia [66].

DA neurotransmission abnormality, either pre- or postsynaptic (e.g., increase of D2 receptor density), disrupts striatal function. The striatum is thought to contain three

functional domains: the sensorimotor, associative, and limbic domains, which approximately correspond to the dorsolateral, dorsomedial, and ventral striatum, respectively (Fig. 1a) [67, 68]. Acting as an integrative hub, associative striatum receives inputs from nearly the entire cortex and connects with the midbrain. Therefore, an aberrant striatal DA signaling elicited by the overexpression of VPAC2 in the DA receptor-expressing neurons can disrupt the integrative hub function of associative striatum and impair the cortical flow of information across cortical–striatal–pallido–thalamo–cortical loops to affect cognitive and affective processes implicated in the pathophysiology of schizophrenia [21].

Currently, the cortical hypodopaminergic function is the leading hypothesis that explains cognitive impairments in schizophrenia. However, in high-risk individuals for schizophrenia, frontal cortex activation during working memory was shown to correlate inversely with associative striatum DA synthesis capacity [69]. Electric or pharmacological activation/inhibition of the striatum in rodents and primates leads to disruptions of spatial working memory [70]. Elegant genetic dissection from Kellendonk et al. [23, 24]. established a causal role of the striatum in cognitive deficits by selectively overexpressing D2 receptors only in the striatum, consequently leading to working memory deficits and perturbation of the prefrontal cortical DA system. Thus, the disruption of striatal function may underlie cognitive deficits. Furthermore, different regions of the striatum have also been implicated in sensorimotor gating deficits and social function [53, 71], and negative symptoms related to impaired reward-based learning [72, 73]. Finally, the striatal abnormality may disrupt the function of the thalamus via the cortical–striatal–pallido–thalamo–cortical loops. Recent mouse genetic studies from Chun et al. showed the aberrant elevation of D2 receptor disrupts thalamic inputs to the auditory cortex in multiple schizophrenia animal models [74], implicating a pathogenic role of the thalamocortical disruption in positive symptoms of schizophrenia. In summary, our model can facilitate the more sophisticated genetic dissection to determine whether primary striatal abnormalities exist in schizophrenia, moreover, when/where/how the striatal function is disrupted and its link to neurochemical and behavioral manifestations of schizophrenia.

Future directions

While our genetic dissection revealed a striking pathogenic role of VIPR2 CNV in the D1 receptor-expressing dSPNs, as shown in Fig. 5b, D1 receptor is expressed in brain regions/cell types far beyond the striatal dSPNs. Our current results could not rule out the disruption of cortical or thalamic excitatory inputs to the striatum due to the VIPR2 overexpression in these regions. In fact, due to the pleiotropic effects of VIP signaling in the whole body, it is difficult to pinpoint the non-cell autonomous role of the VIPR2 CNV., e.g., pathogenic of the VIPR2 ligands, or VIPR2 expression in glia, and even in peripheral immune cells. Thus, the current results will serve as a critical first step that enables future studies employing multiple Cre lines to delete VIPR2 in a combination of cell types to dissect a possible complex pathogenic role of cell–cell interaction, e.g., corticostriatal or thalamostriatal connectivity. Furthermore, to pinpoint the precise time window when the PKA signaling can disrupt brain development, inducible conditional genetics with tamoxifen-inducible Cre recombinase can be used to delete VIPR2 CNV in developmental or adult stages.

Our humanized CNV model also provides an ideal in vivo platform to test therapeutic interventions, e.g., human VPAC2 specific antagonists [75], or search for therapeutics specifically targeting Gαs GPCR /cAMP/PKA signaling. Finally, to explore a therapeutic strategy that can provide long-term remediation of CNV related neurodevelopmental deficits on cognitive circuits, as a proof-of-principle, Cas9 guided by sgRNA can be employed to delete the whole duplicated human VIPR2 genomic region in VIPR2 CNV mice. Taken together, the impact of the study will go beyond the rare cases of carriers with VIPR2 CNVs and this approach affords new mechanistic insights and new therapeutic strategies for nonfamilial (sporadic) schizophrenia patients and broad CNV related neurodevelopmental disorders.

Acknowledgements The project was supported by a NARSAD young investigator award from the Brain & Behavior Research Foundation and a Center for Excellence in Arthritis and Rheumatology grant from LSUHSC to X-HL. X-HL conceived the idea, designed the experiments, and wrote the manuscript. XWY provided valuable guidance in the study, assisting in interpreting the findings, and modifying the manuscript. XWY and NEG served as mentors for the NARSAD award. XT performed most of the behavioral and pathologic studies in Figs. 1–5 and Supplementary Figs. S2–12. BL at LSUHSC performed the HPLC experiment. AR, MWE-S, AB, IVS, and KH performed some behavioral and pathologic studies. Dr Rebecca Berdeaux from the Department of Integrative Biology and Pharmacology, McGovern Medical School at The University of Texas Health Science Center at Houston generously provided CRE-LUC knockin mice. RLK provided open filed, rotarod behavioral equipment and synaptophysin antibody.

Compliance with ethical standards

Conflict of interest The authors declare that they have no conflict of interest.

References

1. Feuk L, Carson AR, Scherer SW. Structural variation in the human genome. Nat Rev Genet. 2006;7:85–97.

2. Malhotra D, Sebat J. CNVs: harbingers of a rare variant revolution in psychiatric genetics. Cell. 2012;148:1223–41.
3. Rice AM, McLysaght A. Dosage sensitivity is a major determinant of human copy number variant pathogenicity. Nat Commun. 2017;8:14366.
4. Andrews T, Honti F, Pfundt R, de Leeuw N, Hehir-Kwa J, Vulto-van Silfhout A, et al. The clustering of functionally related genes contributes to CNV-mediated disease. Genome Res. 2015;25:802–13.
5. Rippey C, Walsh T, Gulsuner S, Brodsky M, Nord AS, Gasperini M, et al. Formation of chimeric genes by copy-number variation as a mutational mechanism in schizophrenia. Am J Hum Genet. 2013;93:697–710.
6. Nestler EJ, Hyman SE. Animal models of neuropsychiatric disorders. Nat Neurosci. 2010;13:1161–9.
7. Vacic V, McCarthy S, Malhotra D, Murray F, Chou HH, Peoples A, et al. Duplications of the neuropeptide receptor gene VIPR2 confer significant risk for schizophrenia. Nature. 2011;471:499–503.
8. Levinson DF, Duan J, Oh S, Wang K, Sanders AR, Shi J, et al. Copy number variants in schizophrenia: confirmation of five previous findings and new evidence for 3q29 microdeletions and VIPR2 duplications. Am J Psychiatry. 2011;168:302–16.
9. Li Z, Chen J, Xu Y, Yi Q, Ji W, Wang P, et al. Genome-wide analysis of the role of copy number variation in schizophrenia risk in Chinese. Biol Psychiatry. 2016;80:331–7.
10. Cnv, Schizophrenia Working Groups of the Psychiatric Genomics C, Psychosis Endophenotypes International C. Contribution of copy number variants to schizophrenia from a genome-wide study of 41,321 subjects. Nat Genet. 2017;49:27–35.
11. Harmar AJ, Fahrenkrug J, Gozes I, Laburthe M, May V, Pisegna JR, et al. Pharmacology and functions of receptors for vasoactive intestinal peptide and pituitary adenylate cyclase-activating polypeptide: IUPHAR review 1. Br J Pharmacol. 2012;166:4–17.
12. Hill JM. Vasoactive intestinal peptide in neurodevelopmental disorders: therapeutic potential. Curr Pharm Des. 2007;13:1079–89.
13. Ago Y, Condro MC, Tan YV, Ghiani CA, Colwell CS, Cushman JD, et al. Reductions in synaptic proteins and selective alteration of prepulse inhibition in male C57BL/6 mice after postnatal administration of a VIP receptor (VIPR2) agonist. Psychopharmacology. 2015;232:2181–9.
14. Quik M, Iversen LL, Bloom SR. Effect of vasoactive intestinal peptide (VIP) and other peptides on cAMP accumulation in rat brain. Biochem Pharmacol. 1978;27:2209–13.
15. Weiss S, Sebben M, Kemp DE, Bockaert J. Vasoactive intestinal peptide actions on cyclic AMP levels in cultured striatal neurons. Peptides. 1986;7 Suppl 1:187–92.
16. Girault JA, Shalaby IA, Rosen NL, Greengard P. Regulation by cAMP and vasoactive intestinal peptide of phosphorylation of specific proteins in striatal cells in culture. Proc Natl Acad Sci USA. 1988;85:7790–4.
17. Girault JA, Horiuchi A, Gustafson EL, Rosen NL, Greengard P. Differential expression of ARPP-16 and ARPP-19, two highly related cAMP-regulated phosphoproteins, one of which is specifically associated with dopamine-innervated brain regions. J Neurosci. 1990;10:1124–33.
18. Greengard P, Allen PB, Nairn AC. Beyond the dopamine receptor: the DARPP-32/protein phosphatase-1 cascade. Neuron. 1999;23:435–47.
19. Taylor DP, Pert CB. Vasoactive intestinal polypeptide: specific binding to rat brain membranes. Proc Natl Acad Sci USA. 1979;76:660–4.
20. Vertongen P, Schiffmann SN, Gourlet P, Robberecht P. Autoradiographic visualization of the receptor subclasses for vasoactive intestinal polypeptide (VIP) in rat brain. Peptides. 1997;18:1547–54.
21. McCutcheon RA, Abi-Dargham A, Howes OD. Schizophrenia, dopamine and the striatum: from biology to symptoms. Trends Neurosci. 2019; 42(3): 205–220.
22. Kesby JP, Eyles DW, McGrath JJ, Scott JG. Dopamine, psychosis and schizophrenia: the widening gap between basic and clinical neuroscience. Transl Psychiatry. 2018;8:30.
23. Simpson EH, Kellendonk C, Kandel E. A possible role for the striatum in the pathogenesis of the cognitive symptoms of schizophrenia. Neuron. 2010;65:585–96.
24. Kellendonk C, Simpson EH, Polan HJ, Malleret G, Vronskaya S, Winiger V, et al. Transient and selective overexpression of dopamine D2 receptors in the striatum causes persistent abnormalities in prefrontal cortex functioning. Neuron. 2006;49:603–15.
25. Goto A, Nakahara I, Yamaguchi T, Kamioka Y, Sumiyama K, Matsuda M, et al. Circuit-dependent striatal PKA and ERK signaling underlies rapid behavioral shift in mating reaction of male mice. Proc Natl Acad Sci USA. 2015;112:6718–23.
26. Kozorovitskiy Y, Peixoto R, Wang W, Saunders A, Sabatini BL. Neuromodulation of excitatory synaptogenesis in striatal development. Elife 2015;4:10111.
27. Shneider Y, Shtrauss Y, Yadid G, Pinhasov A. Differential expression of PACAP receptors in postnatal rat brain. Neuropeptides. 2010;44:509–14.
28. Usdin TB, Bonner TI, Mezey E. Two receptors for vasoactive intestinal polypeptide with similar specificity and complementary distributions. Endocrinology. 1994;135:2662–80.
29. Sheward WJ, Lutz EM, Harmar AJ. The distribution of vasoactive intestinal peptide2 receptor messenger RNA in the rat brain and pituitary gland as assessed by in situ hybridization. Neuroscience. 1995;67:409–18.
30. Michel MC, Wieland T, Tsujimoto G. How reliable are G-protein-coupled receptor antibodies? Naunyn-Schmiede's Arch Pharmacol. 2009;379:385–8.
31. An S, Tsai C, Ronecker J, Bayly A, Herzog ED. Spatiotemporal distribution of vasoactive intestinal polypeptide receptor 2 in mouse suprachiasmatic nucleus. J Comp Neurol. 2012;520:2730–41.
32. Miller JE, Granados-Fuentes D, Wang T, Marpegan L, Holy TE, Herzog ED. Vasoactive intestinal polypeptide mediates circadian rhythms in mammalian olfactory bulb and olfaction. J Neurosci. 2014;34:6040–6.
33. Gerfen CR, Paletzki R, Heintz N. GENSAT BAC cre-recombinase driver lines to study the functional organization of cerebral cortical and basal ganglia circuits. Neuron. 2013;80:1368–83.
34. Harris JA, Hirokawa KE, Sorensen SA, Gu H, Mills M, Ng LL, et al. Anatomical characterization of Cre driver mice for neural circuit mapping and manipulation. Front Neural Circuits. 2014;8:76.
35. Schulz S, Mann A, Novakhov B, Piggins HD, Lupp A. VPAC2 receptor expression in human normal and neoplastic tissues: evaluation of the novel MAB SP235. Endocr Connect. 2015;4:18–26.
36. Schulz S, Rocken C, Mawrin C, Weise W, Hollt V, Schulz S. Immunocytochemical identification of VPAC1, VPAC2, and PAC1 receptors in normal and neoplastic human tissues with subtype-specific antibodies. Clin Cancer Res. 2004;10:8235–42.
37. Tamura M, Mukai J, Gordon JA, Gogos JA. Developmental inhibition of Gsk3 rescues behavioral and neurophysiological deficits in a mouse model of schizophrenia predisposition. Neuron. 2016;89:1100–9.
38. Mena A, Ruiz-Salas JC, Puentes A, Dorado I, Ruiz-Veguilla M, De la Casa LG, et al. Reduced prepulse inhibition as a biomarker of schizophrenia. Front Behav Neurosci. 2016;10:202.
39. Valsamis B, Schmid S. Habituation and prepulse inhibition of acoustic startle in rodents. J Vis Exp. 2011;55:e3446.
40. Kaidanovich-Beilin O, Lipina T, Vukobradovic I, Roder J, Woodgett JR. Assessment of social interaction behaviors. J Vis Exp. 2011: 2473.
41. Hiroi N, Zhu H, Lee M, Funke B, Arai M, Itokawa M, et al. A 200-kb region of human chromosome 22q11.2 confers antipsychotic-responsive behavioral abnormalities in mice. Proc Natl Acad Sci USA. 2005;102:19132–7.

42. Yang XW, Gong S. An overview on the generation of BAC transgenic mice for neuroscience research. Curr. Protoc. Neurosci. 2005; Chapter 5: 5.20.1–5.20.11.
43. Stojanovic T, Orlova M, Sialana FJ, Hoger H, Stuchlik S, Milenkovic I, et al. Validation of dopamine receptor DRD1 and DRD2 antibodies using receptor deficient mice. Amino Acids. 2017;49:1101–9.
44. Yin HH, Knowlton BJ. Contributions of striatal subregions to place and response learning. Learn Mem. 2004;11:459–63.
45. Laruelle M. Imaging dopamine transmission in schizophrenia. A review and meta-analysis. Q J Nucl Med. 1998;42:211–21.
46. Kulkosky PJ, Doyle JS, Cook VI, Glazner GW, Foderaro MA. Vasoactive intestinal peptide: behavioral effects in the rat and hamster. Pharmacol, Biochem, Behav. 1989;34:387–93.
47. Akhmedov D, Mendoza-Rodriguez MG, Rajendran K, Rossi M, Wess J, Berdeaux R. Gs-DREADD knock-in mice for tissue-specific, temporal stimulation of cyclic AMP signaling. Mol Cell Biol. 2017;37:e00584–16.
48. Wojcik SM, Rhee JS, Herzog E, Sigler A, Jahn R, Takamori S, et al. An essential role for vesicular glutamate transporter 1 (VGLUT1) in postnatal development and control of quantal size. Proc Natl Acad Sci USA. 2004;101:7158–63.
49. Nakamura KC, Fujiyama F, Furuta T, Hioki H, Kaneko T. Afferent islands are larger than mu-opioid receptor patch in striatum of rat pups. Neuroreport. 2009;20:584–8.
50. Lu XH. Genetically-directed sparse neuronal labeling in BAC transgenic mice through mononucleotide repeat frameshift. Sci Rep. 2017;7:43915.
51. Caille I, Dumartin B, Le Moine C, Begueret J, Bloch B. Ontogeny of the D1 dopamine receptor in the rat striatonigral system: an immunohistochemical study. Eur J Neurosci. 1995; 7:714–22.
52. Goldman-Rakic PS, Castner SA, Svensson TH, Siever LJ, Williams GV. Targeting the dopamine D1 receptor in schizophrenia: insights for cognitive dysfunction. Psychopharmacology. 2004;174:3–16.
53. Rodrigues S, Salum C, Ferreira TL. Dorsal striatum D1-expressing neurons are involved with sensorimotor gating on prepulse inhibition test. J Psychopharmacol. 2017; https://doi.org/10.1177/0269881116686879.
54. Madisen L, Zwingman TA, Sunkin SM, Oh SW, Zariwala HA, Gu H, et al. A robust and high-throughput Cre reporting and characterization system for the whole mouse brain. Nat Neurosci. 2010;13:133–40.
55. Nelson KB, Grether JK, Croen LA, Dambrosia JM, Dickens BF, Jelliffe LL, et al. Neuropeptides and neurotrophins in neonatal blood of children with autism or mental retardation. Ann Neurol. 2001;49:597–606.
56. Liu X, Li Z, Fan C, Zhang D, Chen J. Genetics implicate common mechanisms in autism and schizophrenia: synaptic activity and immunity. J Med Genet. 2017;54:511–20.
57. Stefansson H, Meyer-Lindenberg A, Steinberg S, Magnusdottir B, Morgen K, Arnarsdottir S, et al. CNVs conferring risk of autism or schizophrenia affect cognition in controls. Nature. 2014;505:361–6.
58. Birnbaum R, Weinberger DR. Genetic insights into the neurodevelopmental origins of schizophrenia. Nat Rev Neurosci. 2017;18:727–40.
59. Wang N, Gray M, Lu XH, Cantle JP, Holley SM, Greiner E, et al. Neuronal targets for reducing mutant huntingtin expression to ameliorate disease in a mouse model of Huntington's disease. Nat Med. 2014;20:536–41.
60. Arnsten AF. Catecholamine influences on dorsolateral prefrontal cortical networks. Biol Psychiatry. 2011;69:e89–99.
61. Kelly MP, Stein JM, Vecsey CG, Favilla C, Yang X, Bizily SF, et al. Developmental etiology for neuroanatomical and cognitive deficits in mice overexpressing Galphas, a G-protein subunit genetically linked to schizophrenia. Mol Psychiatry. 2009;14:398–415, 347.
62. Moyer CE, Shelton MA, Sweet RA. Dendritic spine alterations in schizophrenia. Neuroscience Lett. 2014;601:46–53.
63. Kozorovitskiy Y, Saunders A, Johnson CA, Lowell BB, Sabatini BL. Recurrent network activity drives striatal synaptogenesis. Nature. 2012;485:646–50.
64. Kegeles LS, Abi-Dargham A, Frankle WG, Gil R, Cooper TB, Slifstein M, et al. Increased synaptic dopamine function in associative regions of the striatum in schizophrenia. Arch Gen Psychiatry. 2010;67:231–9.
65. Howes OD, Williams M, Ibrahim K, Leung G, Egerton A, McGuire PK, et al. Midbrain dopamine function in schizophrenia and depression: a post-mortem and positron emission tomographic imaging study. Brain. 2013;136:3242–51.
66. Brunelin J, Fecteau S, Suaud-Chagny MF. Abnormal striatal dopamine transmission in schizophrenia. Curr Med Chem. 2013; 20:397–404.
67. Balleine BW, Delgado MR, Hikosaka O. The role of the dorsal striatum in reward and decision-making. J Neurosci. 2007;27:8161–5.
68. Yin HH, Knowlton BJ. The role of the basal ganglia in habit formation. Nat Rev Neurosci. 2006;7:464–76.
69. Howes OD. Elevated striatal dopamine function linked to prodromal signs of schizophrenia. Arch Gen Psychiatry. 2009;66:13–20.
70. Balleine BW, O'Doherty JP. Human and rodent homologies in action control: corticostriatal determinants of goal-directed and habitual action. Neuropsychopharmacol. 2010;35:48–69.
71. Baez-Mendoza R, Schultz W. The role of the striatum in social behavior. Front Neurosci. 2013;7:233.
72. Gold JM, Strauss GP, Waltz JA, Robinson BM, Brown JK, Frank MJ. Negative symptoms of schizophrenia are associated with abnormal effort-cost computations. Biol Psychiatry. 2013;74:130–6.
73. Morris RW, Quail S, Griffiths KR, Green MJ, Balleine BW. Corticostriatal control of goal-directed action is impaired in schizophrenia. Biol Psychiatry. 2015;77:187–95.
74. Chun S, Westmoreland JJ, Bayazitov IT, Eddins D, Pani AK, Smeyne RJ, et al. Specific disruption of thalamic inputs to the auditory cortex in schizophrenia models. Science. 2014;344:1178–82.
75. Chu A, Caldwell JS, Chen YA. Identification and characterization of a small molecule antagonist of human VPAC(2) receptor. Mol Pharm. 2010;77:95–101.